Development of Redox-Active Aluminum Systems: Synthesis and Characterization of Aluminum-α-Diimine Complexes

Bren E. Cole

Candidate for the degree

Bachelor of Sciences

Submitted in partial fulfilment of the requirements for

College Honors

Departmental Distinction in Chemistry & Biochemistry

Christopher Graves, Ph.D.

Ian Rhile, Ph.D.

Brian Jennings, Ph.D.

F. Wilbur Gingrich Library
Special Collections Department
Albright College

Release of Senior Thesis

I hereby deliver, give, and transfer property, rights, interest in and legal rights thereto which I had, have, or may have concerning the Senior Honors Thesis described below to the Special Collections Department of the F. Wilbur Gingrich Library at Albright College as an unrestricted gift. While copyright privileges will remain with me, the author, all privileges to reproduce, disseminate, or otherwise preserve the Senior Honors Thesis are given to the Special Collections Department of the Gingrich Library. I place no restrictions on this gift and hereby indicate this by signing below.

Title: Development of Redox-Active Aluminum Systems: Synthesis and Characterization of Aluminum-α-Diimine Complexes

Signature of Author: Zeke Cole Date: 4-22-14

Printed Name of Author: Bren Ezekiel Cole

Street Address: 830 Melody Lane

City, State, Zip Code: Lebanon, PA 17046

INTRODUCTION

The addition (reduction) and removal (oxidation) of electrons are fundamental processes in chemistry, and such redox transformations are one of the pillars of synthetic chemistry. Metal catalysts rely on these redox events to make and break bonds, with oxidative addition, reductive elimination, and group atom transfer as important examples for which the ability of the metal to change oxidation state facilitates reaction chemistry(1-3).

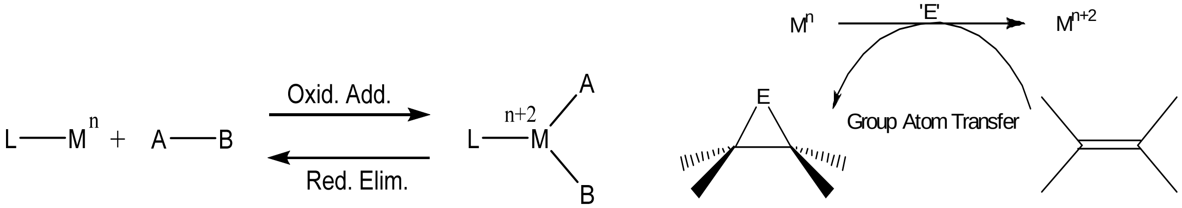

Figure 1. Oxidation states of metal in oxidative addition, reductive elimination, and group atom transfer.

However, traditional redox transformations typically require the use of catalytic systems that employ precious metals that have established redox couples, such as palladium (Pd(0)/Pd(II)), platinum (Pt(0)/Pt(II)), rhodium (Rh(I)/Rh(III)), and iridium (Ir(I)/Ir(III)). Despite these metals being very successful for catalytic processes, their use is limited as they are expensive (particularly for non-Pd) and toxic. For these reasons, recent efforts have been made to develop catalytic systems that employ alternative metal centers. Aluminum is a highly attractive choice for the development of catalytic systems because it is inexpensive, nontoxic, and available commercially in a variety of forms. Aluminum is readily available, accounting for approximately 8% of the mass of the Earth's crust, and costs only \$1.40/kg, making it 10^4-10^5 times less expensive than the precious metals that are often employed for redox catalysis(4-6). Catalytic systems that employ an aluminum center have been developed, but these systems are typically restricted to Lewis-acid catalysis (7), for which the catalyst is responsible for activation of reagents without the transfer of electrons. This is because aluminum chemistries have been defined by its single stable oxidation state, the +3 cation (6). The lack of multiple oxidation states has restricted the use of aluminum complexes for use in catalytic application that require redox events

The Roesky group have prepared rare Al(I)-carbene compounds and used them to conduct two-electron redox transformations with the complexes(8). This project shows that aluminum is capable of facilitating redox processes, but the applicability of these complexes is limited, due to the difficulty of the two electron reduction from Al(III) to Al(I). While the contrasting two electron oxidation is facile, reduction of the Al(III) is extremely difficult. For aluminum complexes to be applicable for redox transformations, complexes able to readily undergo reversible oxidation and reduction chemistries are required.

A potential route for developing a redox-active aluminum system stems from the work of the Heyduk group. They have demonstrated the use of redox-active ligands to create complexes capable of multi-electron transfer processes(9-13). The d^0 metals that were investigated, Ti(IV), Zr(IV), Hf(IV), and Ta(V), are not traditionally capable of performing redox processes, but after coordination of a redox-active ligand set, the overall complexes were able to undergo oxidative addition and reductive elimination. These results set a clear precedent for the ability of a redox-active ligand to extend its electrochemical properties over an entire complex supported by an otherwise redox-inactive metal. Similarly, the Chirik group has demonstrated the same extension of redox activity across an entire complex that is supported by an iron center. In this work, the catalytic systems have been applied to several appropriate chemical processes, including hydrogenation, hydrosilation, and hydroboration of small molecules(14-16). The Chirik group has successfully demonstrated the applicability of these complexes into chemical processes that require electron transfer that is otherwise unavailable to the metal center.

With these reported results in mind, the potential for the development redox-active aluminum systems in this manner is highly attractive. The Berben group has recently explored the use of iminopyridine ligands to synthesize complexes capable of existing in multiple oxidation states(17-21). In this work, by varying the steric demand of the coordinated complexes, Berben and co-workers were able to isolate complexes that spanned multiple oxidation states. When utilizing iminopyridine ligands with an unsubstituted pyridine, complexes of the type (IP)AlX_3, $(IP^-)_2AlX$, and $[M][(IP^{2-})_2Al]$ (X = monoaniionic ligand) were prepared(17-19). Increasing the steric bulk of the pyridine ring in the IP ligands resulted in a series of complexes with one coordinated IP ligand: $(IP^-)AlX_2$ and $(IP^{2-})AlX(OEt_2)$ (X = Cl, Me)(20). Electrochemical data indicated that the complexes were capable of multi-electron processes, and the complexes were successfully utilized as catalysts for reduction reactions involving CO_2(21). These results demonstrate that the use of suitable redox-active ligands can result in the formation of redox-active aluminum systems, and that these complexes can be utilized in catalytic applications.

With precedent for the use of redox-active ligand systems for aluminum established, I decided to investigate the coordination chemistry of α-diimine ligands to an aluminum center, in hopes of creating a novel redox-active aluminum system. The α-diimine ligand was chosen as the redox-active ligand because of its well-established redox chemistry: These ligands can be doubly or singly reduced to form the mono- or dianionic species, respectively(22). Together, neutral and reduced forms of the ligand offer three separate oxidation species for multi-electron transfer to take place, satisfying the demands of typical redox transformations.

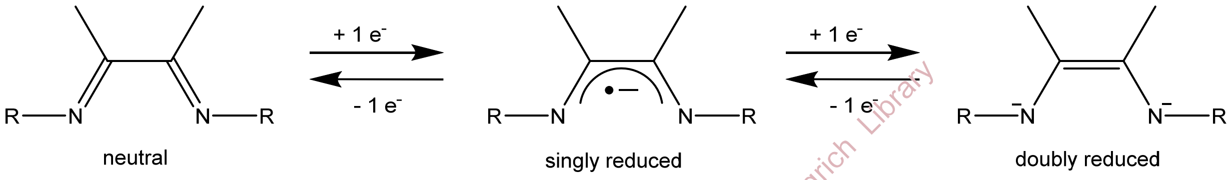

Figure 2. Oxidation states of the α-diimine ligands.

The α-diimine ligand is a useful ligand to use for our goals, because the steric and electronic demands of the ligand can be readily altered by changing the groups located on the aromatic group. This tunability lends itself to a direct investigation into the effects of these parameters on the overall efficiency of the catalytic system. Similar ligands to the α-diimine have been employed in Al(III) systems previously, offering a strong precedent for our proposed chemistry. For instance, the Raston group has utilized the *N*,*N*'-di(*tert*-butyl)-1,4-diazabutadiene ligand to coordinate a doubly reduced ligand and a singly reduced ligand to the Al(III) ion(23). Similarly, the Murphy group has prepared aluminum complexes with the related *N*,*N*'-bis-(2,6-diisopropylphenyl)-1,4-diazabutadiene ligand(24). The Fedushkin group has synthesized aluminum complexes using the (dpp-BIAN$^-$) ligand, demonstrating yet another example of redox-active ligands successfully coordinated to a trivalent aluminum cation(25). Despite all of these examples, the ability of the final aluminum complexes to undergo redox process has not been established.

Herein, I report the synthesis and characterization of aluminum complexes supported by the aryl substituted *N*,*N*'-bis(2,6-diisopropylphenyl)-2,3-dimethyl-1,4-diazabutadiene, **L$_{\text{Dipp}}$** (Figure 3). Synthesis and characterization of the Al-α-diimine complexes were attempted in both the singly and doubly reduced redox states, and a quantum chemical description of the structures was established. The cyclic voltammograms of these complexes exhibit reversible redox events, indicating that the electronic properties of the ligands have been extended to the overall complexes.

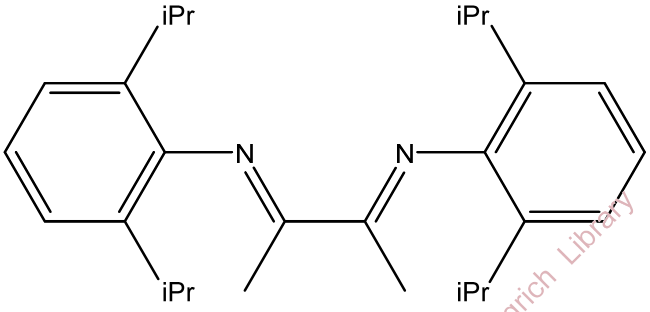

Figure 3. *N*,*N*'-bis(2,6-diisopropylphenyl)-2,3-dimethyl-1,4-diazabutadiene (**L$_{\text{Dipp}}$**)

RESULTS AND DISCUSSION

The α-diimine ligand *N*,*N*'-bis(2,6-diisopropylphenyl)-2,3-dimethyl-1,4-diazabutadiene (**L$_{\text{Dipp}}$**) was prepared according to literature procedure on a 5.0-gram scale in 70% yield (Scheme 1) (26). The ligand was purified by crystallization from cold ethanol. **L$_{\text{Dipp}}$** was characterized by ^{1}H NMR spectroscopy to determine the identity and purity of the ligand (Figure 4). The ^{1}H NMR spectrum shows a downfield aromatic region near 7.2 ppm, the methyl and single hydrogen signals of an isopropyl region around 1.2

ppm and 2.8 ppm, respectively, and shows the amine-backbone methyl groups at 2.2 ppm, confirming the identity of **L_{Dipp}**.

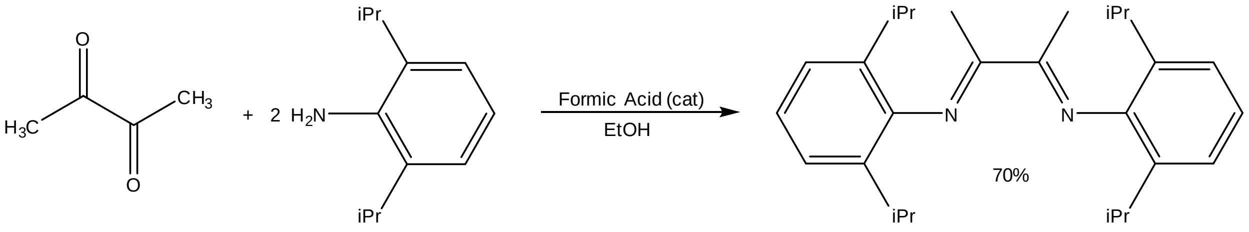

Scheme 1. Preparation of *N*,*N'*-bis(2,6-diisopropylphenyl)-2,3-dimethyl-1,4-diazabutadiene

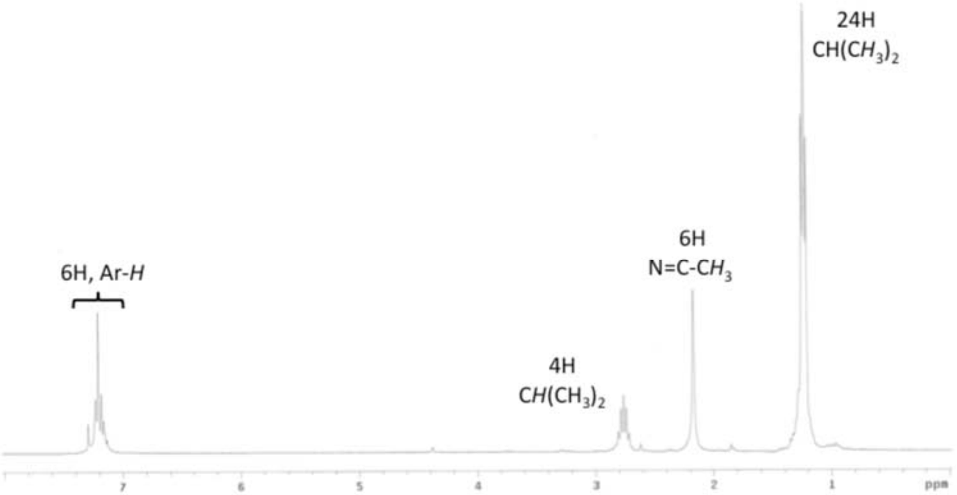

Figure 4. ^{1}H NMR spectrum of **L_{Dipp}** in $CDCl_3$ at 25 °C.

The coordination of the **L_{Dipp}** ligand to aluminum in all three possible oxidation states was attempted. Scheme 2 outlines the synthetic design.

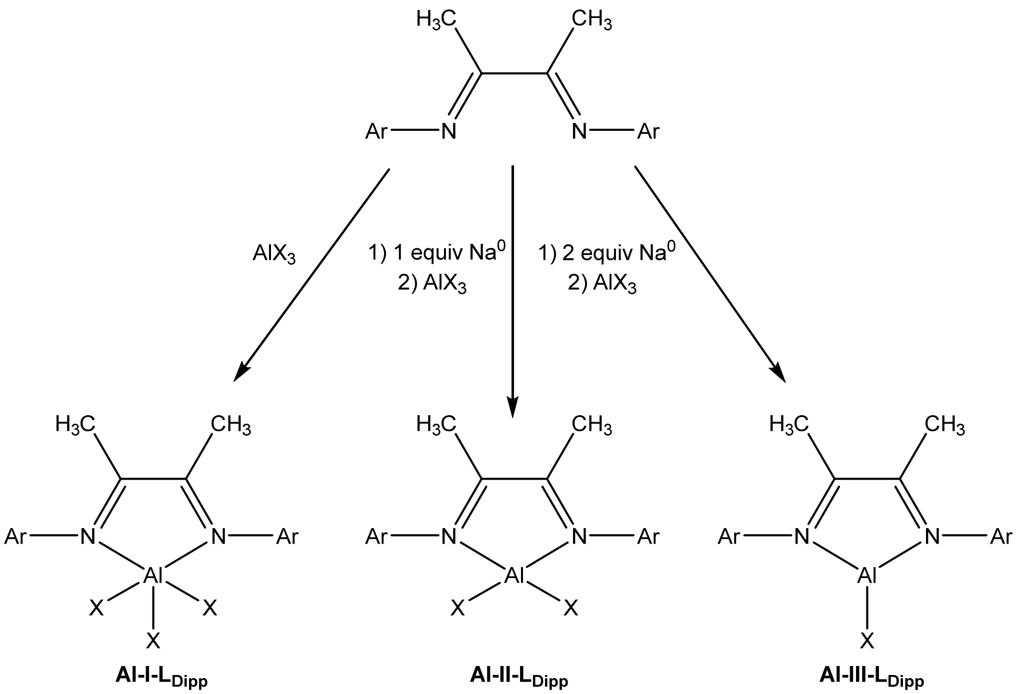

Scheme 2. Synthetic route for coordination of neutral, singly, and doubly reduced Al complexes

Using this reaction scheme, synthesis of the neutral, singly reduced, and doubly reduced Al-α-diimine complexes was attempted. However, reaction of 1 equiv $\mathbf{L_{Dipp}}$ with 1.2 equiv $AlCl_3$ did not result in the intended products. The neutral reaction actually yielded protonated $H\mathbf{L_{Dipp}}^+$ and $AlCl_4^-$ in solution. After meeting unfavorable results with the neutral pathway, the singly reduced reaction was carried out. This reaction was met with success, as reaction of 1 equiv sodium metal with 1 equiv $\mathbf{L_{Dipp}}$, followed by addition of 1.2 equiv $AlCl_3$ resulted in the intended product, **Al-II-L**$_{\mathbf{Dipp}}$. The double reduced pathway did not experience the same success, as reaction of 1 equiv $\mathbf{L_{Dipp}}$ with 2 equiv sodium metal followed by addition of 1.2 equiv $AlCl_3$ did not result in the formation of the intended product. Instead, a mixture of the singly reduced and doubly reduced moieties was often produced. Alternative synthetic pathways were attempted to arrive at the neutral and doubly reduced forms, utilizing oxidizing and reducing agents to accomplish the desired chemistry. However, the neutral and doubly reduced redox forms were not able to be isolated from these reaction chemistry investigations.

Synthesis and Characterization of Aluminum Complex Al-II-L_{Dipp}

Reaction of 1 equiv sodium metal with 1 equiv **L_{Dipp}**, followed by addition of 1.2 equiv $AlCl_3$ resulted in formation of **Al-II-L_{Dipp}** in 77% yield. Characterization of **Al-II-L_{Dipp}** via ^{1}H NMR showed no signals, indicating a paramagnetic species, as was expected.

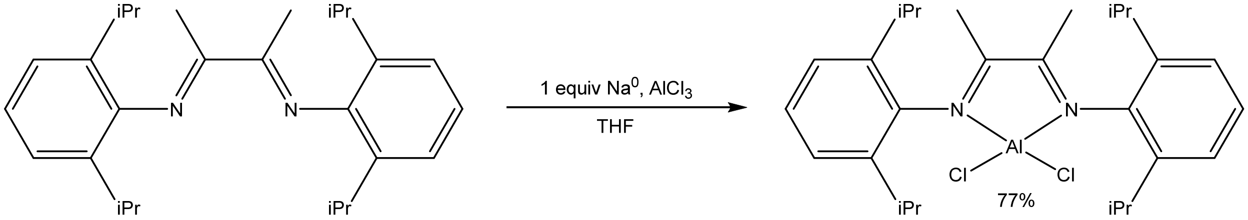

Scheme 3. Preparation of **Al-II-L_{Dipp}**

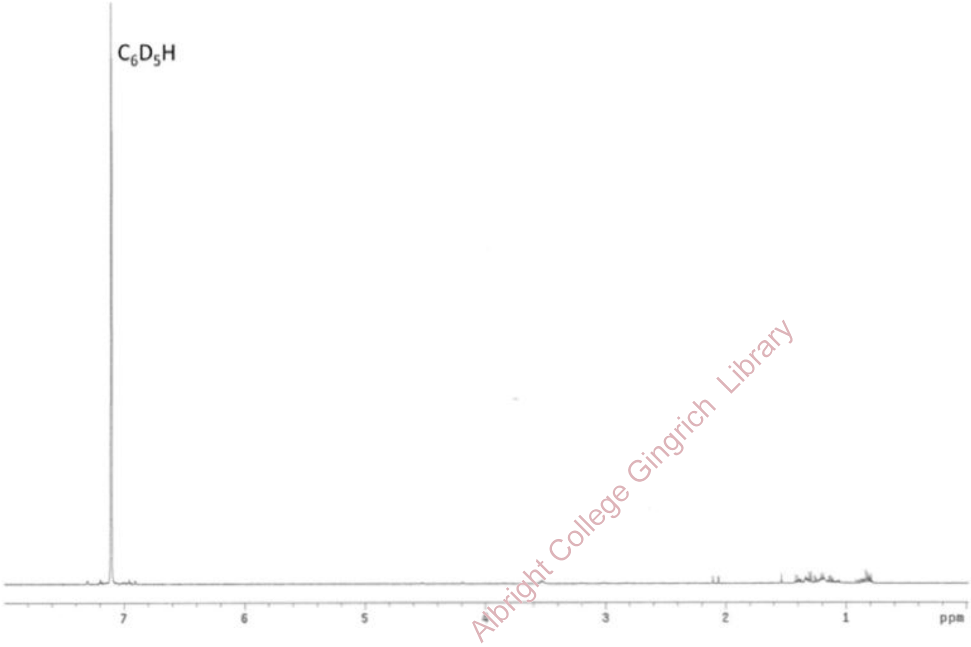

Figure 5. ^{1}H NMR spectrum of **Al-II-L_{Dipp}**.

Solid State Structure of Al-II-L$_{\mathbf{Dipp}}$

The structure of **Al-II-L**$_{\mathbf{Dipp}}$ was confirmed by X-ray crystallography. Single crystals of the complex were grown by recrystallizations in hexane at –25˚C. The solid state structure is shown in Figure 6.

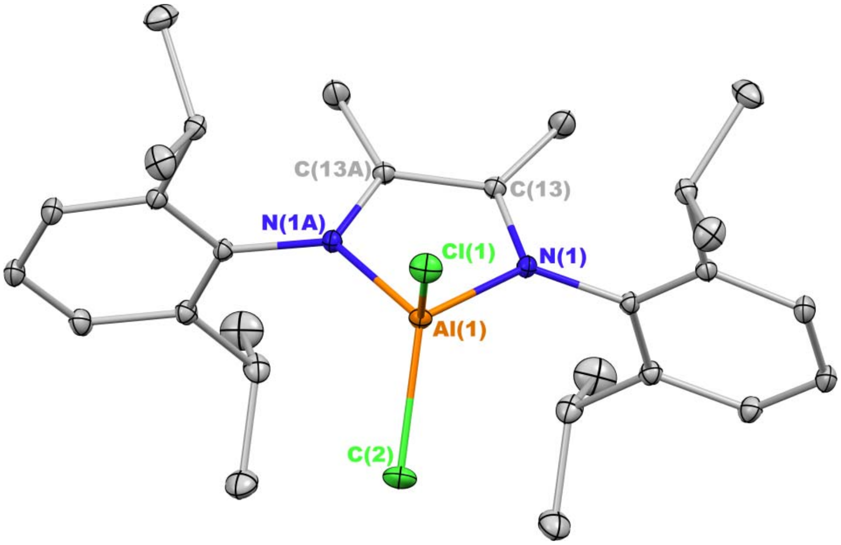

Figure 6. Solid-State structure of **Al-II-L**$_{\mathbf{Dipp}}$.

	Experimental	**Theoretical**
Al–N	1.8733	1.895
Al–Cl	2.1278 2.1078	2.128
C–C$_{\mathbf{backbone}}$	1.466	1.423
C–N$_{\mathbf{imine}}$	1.3456	1.347
N–Al–N	86.77	86.156
N–Al–Cl	113.44 116.14	114.153
Cl–Al–Cl	109.50	111.862

Table 1. Bonding Data for **Al-II-L**$_{\mathbf{Dipp}}$.

The structure is four-coordinate at the aluminum(III) center, with a bidentate α-diimine ligand and two monodentate Cl ligands. This coordination sphere is best described as tetrahedral around the aluminum center, determined by a τ_4 value of 0.92. The bond distances for the N-C-C-N backbone tells us a lot about the electronics of the ligand system. For the above compound, a C–N distance of 1.3456 Å and a C-C distance of 1.466 Å are observed. These measurements correspond to a shortening of the C-N bonds and a lengthening of the C-C bond relative to the neutral $\mathbf{L_{Dipp}}$, which has a C-N bond length of 1.278 Å and a C-C bond length of 1.500 Å (27). These changes in bonding parameters are in agreement with the expected changes that accompany the addition of an electron to the α-diimine ligand, as reported by Yang and co-workers (28). In their $[(L_{Dipp}{}^{-})Ca(\mu_2\text{-}Cl)(THF)_2]_2$ complex, the C-N bond distances are 1.473 Å and 1.379 Å and a C–C distance of 1.354 Å. The bonding metrics also agree well with those found for the $(L_{Diip}{}^{-})AlEt_2$ complex, which had C–N distances of 1.375 Å and 1.390 Å and a C–C distance of 1.391 Å (27).

Density Functional Theory (DFT) Studies

The optimized structures of $\mathbf{Al\text{-}II\text{-}L_{Dipp}}$ and $\mathbf{Al\text{-}III\text{-}L_{Dipp}}$ were generated theoretically using the Gaussian ’09 program, M06 density functional and 6-31+g(d,p) basis set The computational results agree well with the results from X-ray diffraction for the singly reduced complex, as the generated bond parameters bear a close similarity to the X-ray diffraction data (Table 1). The theoretical data shows a shortening of the C–C bond, and a lengthening of the C–N bonds, which is in agreement with the proposed repercussions of adding one or two electrons, respectively, to this system. In both cases, the added electron density is added to an antibonding orbital for the C-N bonds, and a bonding orbital for the C-C bonds, explaining the respective lengthening and shortening of the bonds upon reduction. The SOMO of the singly reduced and the HOMO of the doubly reduced complexes are presented below, respectively in Figure 7.

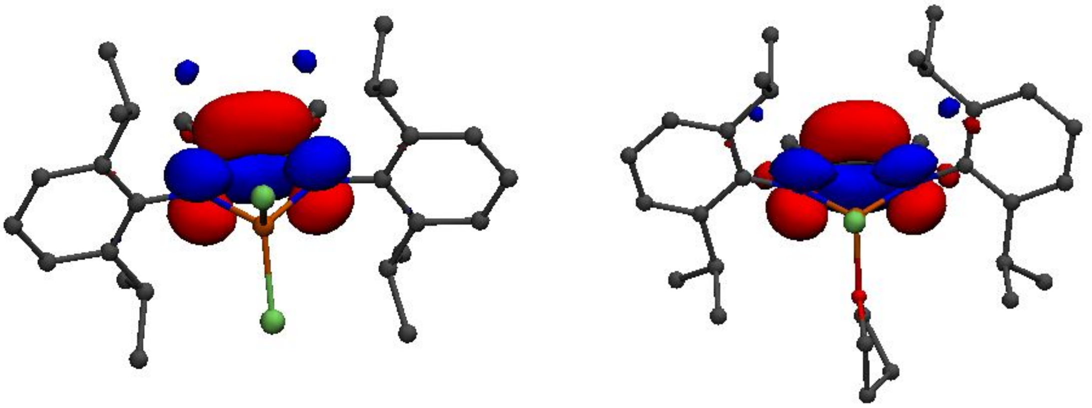

Figure 7. Optimized Structures of **Al-II-L$_{\mathbf{Dipp}}$** and **Al-III-L$_{\mathbf{Dipp}}$**.

The charge distribution on the atoms of the above complexes was also calculated using the natural bonding orbital (NBO) method, shown in Table 2. These studies confirmed that the electron density from the added electron is situated mostly upon the α-diimine ligand, as was expected for this chemistry. In both complexes, the nitrogen binding sites acquire much of the electron density, indicating an anionic character for the ligand.

	Al	**Cl(1)**	**Cl(2)/O(1)**	**C(1)**	**C(2)**	**N(1)**	**N(2)**
Al-II-L$_{\mathbf{Dipp}}$	+1.67947	-0.53221	-0.53221	+0.23166	+0.23166	-0.78422	-0.78422
Al-III-L$_{\mathbf{Dipp}}$	+1.91026	-0.54448	-0.72426	+0.08449	+0.10456	-1.00342	-1.00496

Table 2. Charge Distribution of **Al-II-L$_{\mathbf{Dipp}}$** and **Al-III-L$_{\mathbf{Dipp}}$**

Electrochemistry

The electrochemistry of the singly reduced complex **Al-II-L$_{\mathbf{Dipp}}$** was investigated to determine if all three redox states could be electrochemically accessed. The electrochemistry data was collected in THF with 0.1 M [*n*-Pr$_4$N][BAr^F] (BAr^F = [B(3,5-CF$_3$)$_2$-C$_6$H$_3$)$_4$]$^-$) electrolyte. The cyclic voltammetry (Figure 8) shows that the complex exhibits two independent, clean, and reversible redox waves. These waves can be identifies as the L^{2-}/L$^-$ couple at $E_{1/2}$= –1.34 V and the L$^-$/L^0 couple at $E_{1/2}$= –0.62 V with respect to Fc/Fc$^+$. The experiment. The presence of these two reversible waves is encouraging, as it shows that the aluminum complex is can support all three oxidative states electrochemically and remain stable in all three of those redox states, a key component of a redox-active catalytic system.

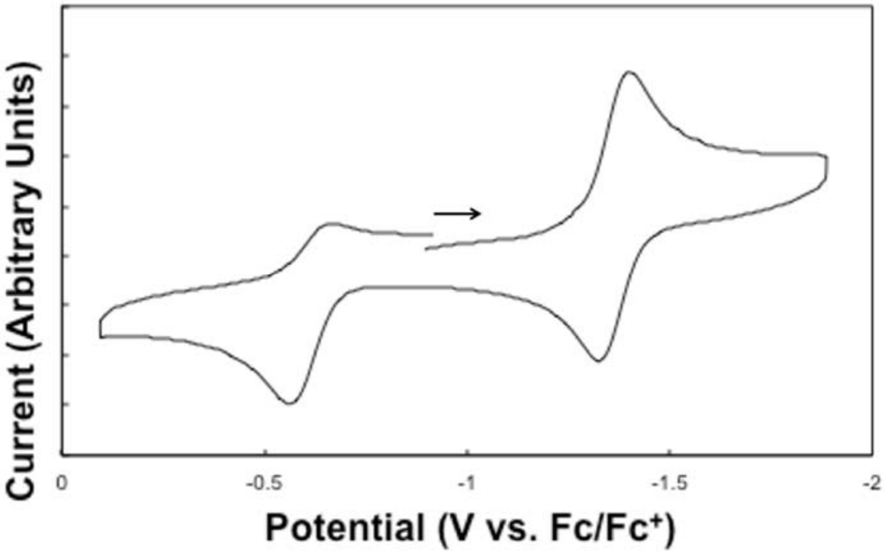

Figure 8. Cyclic Voltammetry of **Al-II-L$_{\mathbf{Dipp}}$**.

CONCLUSIONS

While the synthesis of the Al-α-diimine complexes in all three oxidation states did not occur as smoothly as initially expected, many conclusions were drawn from the work that was accomplished in this project. Coordination of an α-diimine ligand to an aluminum center was presented, and it was demonstrated that the resulting singly-reduced compound was stable across three oxidative states. Coordination of the α-diimine ligand to an aluminum center was shown, for which the α-diimine ligand extends its redox chemistries to the rest of the complex, offering preliminary successes upon which to build a later project. It was also shown through computational studies that the electronic transformations of the complexes are facilitated by the α-diimine ligand, allowing the aluminum center to remain in the +3 oxidation state.

This work laid a foundation for further studies on Al-α-diimine systems, culminating in the investigation of the aluminum complexes supported by the *N*,*N'*-bis[2,4,6-trimethylphenyl]-2,3-dimethyl-

1,4-diazabutadiene, **L_{Mes}** ligand. The resulting Al-L_{Mes} complexes were isolated in both the singly- and doubly-reduced forms. These complexes experienced encouraging results in electrochemistry and characterization studies as well, and show greater promise for representing a set of aluminum complexes that exist in multiple oxidation states.

EXPERIMENTAL SECTION

Physical Measurements

^{1}H and ^{13}C NMR spectra were recorded at ambient temperature in C_6D_6 using a Varian 400 MHz spectrometer (399.78 MHz for ^{1}H, 100.52 MHz for ^{13}C). Chemical shifts were referenced to residual protonated solvent. Elemental analyses were performed at the University of California, Berkeley Microanalytical Facility, on a Perkin-Elmer Series II 2400 CHNS analyzer.

Electrochemical Measurements.

CVs were recorded in a glovebox under a dinitrogen environment using a CH Instruments 620D Electrochemical Analyzer/Workstation with a glassy carbon working electrode, a platinum wire auxiliary electrode, and a silver wire plated with AgCl as a quasi-reference electrode were utilized. Potentials were reported versus Fc/Fc$^+$, which was added as an internal standard for calibration at the end of each run. Solutions employed during these studies were ~3 mM in analyte and 100 mM in [*n*-Pr_4N][BAr^F] (BAr^{F-} = $B(3,5-CF_3)_2-C_6H_3)4^-$) in ~3 mL of THF. All data were collected in a positive-feedback IR compensation mode.

X-ray Structure Determination.

X-ray diffraction data were collected on a Bruker-AXS Kappa APEX II CCD diffractometer with 0.71073 A Mo-Kα radiation. Cell parameters were retrieved using APEX II software and further refined on all observed reflections during integration using SAINT+. The data set was treated with SADABS absorption corrections based on redundant multi-scan data. The structure was solved by direct methods and refined by least-squares method on F2 using the SHELXTL program package. All non-hydrogen atoms were refined with anisotropic displacement parameters and all hydrogen atoms were treated with a riding model.

X-ray structural analysis for 1: A single orange block (0.2 × 0.12 × 0.10 mm^3) was mounted in immersion oil onto a glass fiber and data were collected under a nitrogen stream at 100 K. Systematic absences in the data were consistent with the centrosymmetric, orthorhombic space group *Pnma*. The asymmetric unit contains one half-molecule of **Al-II-L_{Dipp}**, as the molecule lies on a crystallographic mirror plane.

Computational Details.

The structure optimization of 1 and 2 were performed with the Gaussian09, Revision A.1, program using the M06 density functional and the 6-31+g(d,p) basis set. Geometry operations were carried out in C_1 symmetry for **Al-III-L_{Dipp}** and C_{2v} symmetry for **Al-II-L_{Dipp}**. All frequency calculations found no imaginary frequencies, confirming that the optimized structures were minima. Binding analysis was performed using NBO 3 as coded within Gaussian 09. Molecular orbitals were visualized using Visual Molecular Dynamics44 with isosurfaces at ±0.03 a.u.

Preparation of Compounds.

All reactions and manipulations were performed under an inert atmosphere (N_2) using standard Schlenk techniques or in a Vacuum Atmospheres, Inc. Nexus II drybox equipped with a molecular sieves 13X / Q5 Cu-0226S catalyst purifier system. Glassware was dried overnight at 150 °C before use. C_6D_6 was purchased from Sigma Aldrich and was stored over potassium metal prior to use. Tetrahydrofuran, hexanes, pentane, and toluene were purchased from Fisher Scientific. These solvents were sparged for 20 min with dry argon and dried using a commercial two-column solvent purification system comprising columns packed with Q5 reactant and neutral alumina respectively (for hexanes, toluene, and pentane), or two columns of neutral alumina (for THF). Celite was purchased from Sigma-Aldrich and was dried under reduced pressure at 250 °C for 48 h prior to use. The α-diimine ligand **L_{Dipp}** was prepared according to literature procedures(13). [n-Pr_4N][BAr^F] was prepared as reported by Kiplinger et al(29). All other reagents were purchased from commercial sources and used as received.

L_{Dipp}, *N*,*N*'-bis(2,6-diisopropylphenyl)-2,3-dimethyl-1,4-diazabutadiene

Formic acid (10 drops) was added to a stirring solution of butanedione (1.0 g, 11.6 mmol) and 2,6-diisopropylaniline (4.119 g, 23.2 mmol) in ethanol (20 mL). After overnight stirring, the solution turned from yellow to red, and yellow solid precipitated out from the reaction mixture. The crude reaction product was recrystallized from a hot hexane solution at –25 °C, and resulting yellow crystals were filtered over a Celite-padded frit and collected to provide 1.2164 g (70%) of yellow solid.

Al-II-L_{Dipp}

N,*N*'-bis(2,6-diisopropylphenyl)-2,3-dimethyl-1,4-diazabutadiene (0.50 g, 1.23 mmol) in THF (10 mL) was added to a stirring suspension of sodium metal (0.028 g, 1.23 mmol) in THF (25 mL). After 4 h, $AlCl_3$ (0.16 g, 1.23 mmol) was added and the reaction was allowed to stir at room temperature. After 12 h, the reaction was filtered over a Celite-padded frit and volatiles were removed from the pale yellow filtrate under vacuum. The crude reaction product was taken up into hot toluene (25 mL), filtered over a Celite-padded frit and volatiles were removed from the filtrate to provide 0.48 g (77%) of a solid. Crystals suitable for X-ray diffraction were obtained from cooling a saturated hexane solution at –25 °C. Anal. Calcd for $C_{28}H_{40}AlCl_2N_2$: C, 66.92; H, 8.02; N, 5.57. Found: C, 67.45; H, 8.07; N, 5.25.

REFERENCES

(1) Ozerov, Oleg V. *Chemical Society Reviews*. **2009**, 38, 83-88.

(2) Vedernikov, Andrei N. *Topics in Organometallic Chem*. **2010**, 31, 101-121.

(3) Fuchise, Keita; Chen, Yougen; Satoh, Toshifumi; Kakuchi, Toyoji. *Polymer Chem*. **2013**, 4, 4278-4291.

(4) Haynes, W. M., Ed. CRC Handbook of Chemistry and Physics, 91st ed. CRC: Boca Raton, **2010**; p 4-1-4-42.

(5) Rabinovich, D. *Nat. Chem.* **2013**, *5*, 76.

(6) Cotton, F. A.; Wilkinson, G.; Murillo, C. A.; Bochmann, M. *Advanced Inorganic Chemistry*. 6th ed.; John Wiley & Sons, Inc.: New York, **1999**.

(7) Taguchi, T.; Yanai, H. Al(III) Lewis Acids. In *Acid Catalysis in Modern Organic Synthesis*; Yamamoto, H.; Ishihara, K., Eds.; Wiley-VCH: **2008**; Vol. 1, p 241-345.

(8) Cui, C.; Roesky, H. W.; Schmidt, H.-G.; Noltemeyer, M.; Hao, H.; Cimpoesu, F. *Angew. Chem*., Int. Ed. **2000**, 39, 4274-4276.

(9) Haneline, M. R.; Heyduk, A. F.; *J. Am. Chem. Soc.* **2006**, 128, 8410-8411.

(10) Blackmore, K. J.; Ziller, J. W.; Heyduk, A. F. *Inorg. Chem.* **2005**, *44*, 5559-5561.

(11) Haneline, M. R.; Heyduk, A. F. *J. Am. Chem. Soc.* **2006**, *128*, 8410-8411.

(12) Blackmore, K. J.; Lal, N.; Ziller, J. W.; Heyduk, A. F. *J. Am. Chem. Soc.* **2008**, *130*, 2728-2729.

(13) Nguyen, A. I.; Zarkesh, R. A.; Lacy, D. C.; Thorson, M. K.; Heyduk, A. F. *Chem. Sci.* **2011**, *2*, 166-169.

(14) Darmon, J. M.; Stieber, S. C. E.; Sylvester, K. T.; Fernandez, I.; Lobkovsky, E.; Semproni, S. P.; Bill, E.; Wieghardt, K.; DeBeer, S.; Chirik, P. J. *J. Am. Chem. Soc.* **2012**, *134*, 17125-17137.

(15) Bart, S. C.; Lobkovsky, E.; Chirik, P. J. *J. Am. Chem. Soc.* **2004**, *126*, 13794-13807.

(16) Bart, S. C.; Hawrelak, E. J.; Lobkovsky, E.; Chirik, P. J. *Organometallics* **2005**, *24*, 5518-5527.

(17) Myers, T. W.; Berben, L. A. *J. Am. Chem. Soc.* **2011**, *133*, 11865-11867.

(18) Myers, T. W.; Holmes, A. L.; Berben, L. A. *Inorg. Chem.* **2012**, *51*, 8997-9004.

(19) Myers, T. W.; Kazem, N.; Stoll, S.; Britt, R. D.; Shanmugam, M.; Berben, L. A. *J. Am. Chem. Soc.* **2011**, *133*, 8662-8672.

(20) Myers, T. W.; Berben, L. A. *Inorg. Chem.* **2012**, *51*, 1480-1488.

(21) Myers, T. W.; Berben, L. A. *Chem. Commun.* **2013**, *49*, 4175-4177.

(22) Chirik, P. J. *Inorg. Chem.* **2011**, *50*, 9737-9740.

(23) Cloke, F. G. N.; Dalby, C. I.; Henderson, M. J.; Hitchcock, P. B.; Kennard, C. H. L.; Lamb, R. L.; Raston, C. L. *J. Chem. Soc., Chem. Commun.* **1990**, 1394-1396.

(24) Baker, R. J.; Farley, R. D.; Jones, C.; Kloth, M.; Murphy, D. M. *J. Chem. Soc., Dalton Trans.* **2002**, 3844-3850.

(25) Schumann, H.; Hummert, M.; Lukoyanov, A. N.; Fedushkin, I. L. *Organometallics* **2005**, *24*, 3891-3896.

(26) Van, A. B. R.; Glass, J. L.; Wiggins, K. M.; Aarif, A. M.; Louie, J. *J. Org. Chem.* **2009**, *74*, 7935-7942.

(27) Li, J.; Zhang, K.; Huang, H.; Yu, A.; Hu, H.; Cui, H.; Cui, C. *Organometallics* **2013**, *32*, 1630-1635.

(28) Liu, Y.; Zhao, Y.; Yang, X.-J.; Li, S.; Gao, J.; Yang, P.; Xia, Y.; Wu, B. *Organometallics* **2011**, *30*, 1599-1606.

(29) Thomson, R. K.; Scott, B. L.; Morris, D. E.; Kiplinger, J. L. *C. R. Chim.* **2010**, *13*, 790-802.